Available online at www.sciencedirect.com
SCIENCE DIRECT®
Biochemical and Biophysical Research Communications 323 (2004) 24–31
BBRC
www.elsevier.com/locate/ybbrc

Crystal structure of an acidic platelet aggregation inhibitor and hypotensive phospholipase A_2 in the monomeric and dimeric states: insights into its oligomeric state☆

Angelo J. Magro[a,1], Mário T. Murakami[b,1], Silvana Marcussi[c], Andreimar M. Soares[c], Raghuvir K. Arni[b], Marcos R.M. Fontes[a,*]

[a] *Departamento de Física e Biofísica, Instituto de Biociências, UNESP, Botucatu-SP, Brazil*
[b] *Departamento de Física, IBILCE, UNESP, São José do Preto-SP, Brazil*
[c] *Unidade de Biotecnologia, UNAERP, Ribeirão Preto-SP, Brazil*

Received 4 August 2004
Available online 21 August 2004

Abstract

Phospholipases A_2 belong to the superfamily of proteins which hydrolyzes the *sn*-2 acyl groups of membrane phospholipids to release arachidonic acid and lysophospholipids. An acidic phospholipase A_2 isolated from *Bothrops jararacussu* snake venom presents a high catalytic, platelet aggregation inhibition and hypotensive activities. This protein was crystallized in two oligomeric states: monomeric and dimeric. The crystal structures were solved at 1.79 and 1.90 Å resolution, respectively, for the two states. It was identified a Na^+ ion at the center of Ca^{2+}-binding site of the monomeric form. A novel dimeric conformation with the active sites exposed to the solvent was observed. Conformational states of the molecule may be due to the physicochemical conditions used in the crystallization experiments. We suggest dimeric state is one found in vivo.

Keywords: X-ray crystallography; Acidic phospholipase A_2; *Bothrops jararacussu* venom; Platelet aggregation and hypotensive effects; Crystal structure; Oligomeric state; Dimeric phospholipase A_2

Phospholipases A_2 (PLA_2, EC 3.1.1.4) belong to the superfamily of proteins which hydrolyzes the *sn*-2 acyl groups of membrane phospholipids to release arachidonic acid and lysophospholipids. The superfamily of PLA_2s is divided into 11 classes [1], of which five (I, II, III, V, and X) are abundant in a variety of biological fluids, particularly pancreatic secretions, inflammatory exudates, and reptile and arthropod venoms [2]. PLA_2s are the major components of snake venoms, being those of group IIA predominant in *Bothrops* venoms. In addition to their primary catalytic role, snake venoms PLA_2s show other important toxic/pharmacological effects including myonecrosis, neurotoxicity, cardiotoxicity, and hemolytic, hemorrhagic, hypotensive, anticoagulant, platelet aggregation inhibition, and edema-inducing activities [3–5]. Some of these activities correlate with the enzymatic activity and others are completely independent [6,7].

PLA_2s are also one of the enzymes involved in the production of eicosanoids. These molecules have physiological effects at very low concentrations; however, the increasing of their concentration can lead to the state of

☆ *Abbreviations:* PLA_2, phospholipase A_2; BthA-I, acidic phospholipase A_2 from *Bothrops jararacussu* venom; m-BthA-I, monomeric acidic phospholipase A_2 from *Bothrops jararacussu* venom; d-BthA-I, dimeric acidic phospholipase A_2 from *Bothrops jararacussu* venom.

* Corresponding author. Fax: +55 14 38153744.
E-mail address: fontes@ibb.unesp.br (M.R.M. Fontes).

[1] These authors contributed equally to this work.

0006-291X/$ - see front matter © 2004 Elsevier Inc. All rights reserved.
doi:10.1016/j.bbrc.2004.08.046

inflammation [8]. Then, the study of specific PLA_2s inhibitors can be important in the production of structure-based anti-inflammatory agents.

A group of myotoxic Phospholipases A_2 homologues present in the venoms of some species of *Agkistrodon*, *Bothrops*, and *Trimeresurus* (family Viperidae) is characterized by a Lys to Asp substitution of residue 49 [9,10]. The coordination of the Ca^{2+} ion in the PLA_2 calcium-binding loop includes an Asp at position 49 which plays a crucial role in the stabilization of the tetrahedral transition state intermediate in catalytically active phospholipases A_2 [11]. Therefore, the Asp49 to Lys substitution drastically affects the calcium-binding ability of these Lys49-PLA_2 homologues and, as a consequence, they present a very limited catalytic activity.

Many basic Lys49-PLA_2s have been purified from *Bothrops* snake venoms and structurally and functionally characterized [12–18]. However, little is known about the bothropic Asp49-PLA_2s [19–21]. Two basic myotoxic phospholipases A_2, the bothropstoxin-I (Lys49-BthTX-I—catalytic inactive) and II (Asp49-BthTX-II—low catalytic activity), have been isolated from *Bothrops jararacussu* venom and characterized [15,18,22,23]. BthA-I is three to four times more active catalytically than BthTX-II and other basic Asp49 PLA_2 from *Bothrops* venoms, however, it is not myotoxic, cytotoxic or lethal. Although it showed no toxic activity, it was able to induce time-independent edema. In addition, BthA-I caused a hypotensive response in rats and inhibited platelet aggregation [24]. Catalytic, desintegrin, and pharmacological activities were abolished by chemical modification with *p*-bromophenacyl bromide, which covalently binds to His48 of the catalytic site [24]. In order to better understand the structure–function relationship of these bothropic proteins, the cDNA sequence cloning, functional expression crystallization, and X-ray diffraction data of BthA-I-PLA_2 were recently described [24–26].

In this paper, we described the high resolution crystal structures of BthA-I-PLA_2 in two oligomeric states: monomeric and dimeric.

Table 1
X-ray data collection and refinement statistics

	d-BthA-I	m-BthA-I
Unit cell (Å)	$a = 33.19$ $b = 63.14$ $c = 47.40$ $\beta = 102.3$	$a = 39.98$ $b = 53.99$ $c = 90.46$
Space group	$P2_1$	$C222_1$
Resolution (Å)	29.7–1.9 (2.02–1.9)[a]	30.0–1.79 (1.84–1.79)[a]
Unique reflections	14,151 (2084)[a]	9034 (507)[a]
Completeness (%)	93.3 (87.7)[a]	94.3 (80.1)[a]
R_{merge}[b] (%)	4.5 (29.3)[a]	4.6 (15.3)[a]
$I/\sigma(I)$	20.1 (5.0)[a]	22.1 (6.0)[a]
Redundancy	3.5 (3.4)[a]	5.7(1.2)[a]
R_{Cryst}[c] (%)	19.0 (23.8)[a]	18.6 (24.6)[a]
R_{free}[d] (%)	24.7 (28.5)[a]	25.5 (33.8)[a]
Number of non-hydrogen atoms:		
Protein	1900	949
Water	381	144
Mean *B* factor (Å^2)[e]		
Overall	27.8	23.2
Main chain atoms	34.6	17.4
Side chain atoms	35.6	19.4
Water molecules	49.0	27.9
Na^+ ion	38.1	—
R.m.s deviations from ideal values[e]		
Bond lengths (Å)	0.005	0.018
Bond angles (°)	1.3	1.9
Ramachandran plot[f] (%)		
Residues in most favored region	90.7	92.2
Residues in additional allowed region	9.3	7.8
Residues in generously/disallowed regions	0.0	0.0
Coordinate error (Å)[e]		
Luzzati plot (cross-validated Luzzati plot)	0.20 (0.28)	0.18 (0.38)
SIGMAA (cross-validated SIGMAA)	0.22 (0.22)	0.11 (0.11)

[a] Numbers in parentheses are for the highest resolution shell.

[b] $R_{merge} = \sum_{hkl}(\sum_i(|I_{hkl,i} - \langle I_{hkl}\rangle|))/\sum_{hkl,i}\langle I_{hkl}\rangle$, where $I_{hkl,i}$ is the intensity of an individual measurement of the reflection with Miller indices *h*, *k*, and *l*, and $\langle I_{hkl}\rangle$ is the mean intensity of that reflection. Calculated for $I > -3\sigma(I)$.

[c] $R_{cryst} = \sum_{hkl}(||Fobs_{hkl}| - |Fcalc_{hkl}||)/|Fobs_{hkl}|$, where $|Fobs_{hkl}|$ and $|Fcalc_{hkl}|$ are the observed and calculated structure factor amplitudes.

[d] R_{free} is equivalent to R_{cryst} but calculated with reflections (5%) omitted from the refinement process.

[e] Calculated with the program CNS [30].

[f] Calculated with the program PROCHECK [34].

Materials and methods

Isolation, cDNA cloning, and sequencing. BthA-I-PLA_2 was isolated from *B. jararacussu* snake venom by ion-exchange chromatography on CM-Sepharose followed by reverse phase chromatography on a RP-HPLC C-18 column [24]. The amino acid sequence of BthA-I-PLA_2 was deduced from the cDNA sequence and deposited in GenBank (AY145836) [25,26].

Crystallization and data collection. BthA-I-PLA_2 was crystallized in two different conditions: 0.2 M ammonium sulfate and 22% (w/v) polyethylene glycol 6000 (d-BthA-I) [24]; and 0.1 M sodium acetate (pH 4.6) and 28% polyethylene glycol 4000 (m-BthA-I). Lyophilized sample of BthA-I-PLA_2 was dissolved in ultra-pure water at a concentration of 10 and 12 mg/mL, respectively, for crystals of m-BthA-I and d-BthA-I. The crystals were flash-frozen (15% glycerol for m-BthA-I) and diffraction data were collected at a wavelength of 1.38 Å (at 100 K) using a Synchrotron Radiation Source (LNLS, Campinas, Brazil). Diffraction intensities were measured using a MAR 345 imaging-plate detector and were reduced and processed using the HKL suite [27]. The data sets are 94.3% and 93.3% complete at 1.79 and 1.9 Å resolution with $R_{merge} = 4.6\%$ and 4.5% for m-BthA-I and d-BthA-I, respectively. The m-BthA-I crystals belong to the space group $C222_1$ and for m-BthA-I to the space group $P2_1$. Data processing statistics are presented in Table 1.

Structure determination and refinement. The crystal structures of m-BthA-I and d-BthA-I were solved by the Molecular Replacement Method using the program AMoRe [28] and the coordinates of the Lys49-PLA_2 from *Agkistron piscivorus piscivorus* (PDB code 1VAP) [29]. The model choice was based on the best results of correlation and *R* factor from the AMoRe program. After a cycle of simulated annealing refinement using the CNS program [30], the electron densities were inspected and the amino acid sequence as obtained from the cDNA of BthA-I [25,26] was inserted for both m-BthA-I and d-BthA-I. The modeling process was always performed by manually rebuilding with the "O" program [31]. Electron density maps calculated with coefficients $3|F_{obs}| - 2|F_{calc}|$ and simulated annealing omit maps calculated with analogous coefficients were generally used. The model was improved, as judged by the free *R* factor [32], through rounds of crystallographic refinement (positional and restrained isotropic individual *B* factor refinement, with an overall anisotropic temperature factor and bulk solvent correction) using the CNS program [30], and manual rebuilding with the "O" program [31]. Solvent molecules were added and refined also with the program CNS [30]. In the last stages of refinement of m-BthA-I the program REFMAC 5.0 was used [33].

The refinement converged to *R* and free *R* factors of 18.3% and 24.3%; 19.0% and 24.7%, respectively, for m-BthA-I and d-BthA-I (see Table 1 for explanation of *R* factors). The final models comprise 950 protein atoms and 144 water molecules for m-BthA-I, and 1900 protein atoms and 381 water molecules for d-BthA-I. The refinement statistics are shown in Table 1. For molecular comparisons of the Lys49-PLA_2 structures, the "O" program [31] was used with only the C^{α} coordinates. The quality of the model was checked with the PROCHECK program [34]. The coordinates have been deposited in the RCSB Protein Data Bank with ID code 1UMV and 1U73, respectively, for m-BthA-I and d-BthA-I.

Results

The structures showed overall stereochemistry better than expected for an average structure at the same resolution, where no residue was found in the disallowed or generously allowed regions of Ramachandran plot, and with the overall Procheck *G* factor of 0.4 and −0.1 for d-BthA-I and m-BthA-I, respectively [34].

The m-BthA-I and d-BthA-I monomers are very similar to other class IIA PLA_2 structures. As is usual for other proteins of this class, there are seven disulfide bridges and the main secondary structural elements are conserved. The structure is composed of: (i) N-terminal α-helix 1, (ii) Ca^{2+}-binding loop, (iii) two anti-parallel α-helixes 2 and 3, (iv) short two-stranded anti-parallel β-sheet (β-wing), and (v) C-terminal loop (Fig. 1A).

The monomers of m-BthA-I and d-BthA-I are essentially identical, where the r.m.s. deviation of C^{α} atoms is 0.49 Å for both superposition of d-BthA-I monomer A and m-BthA-I, and d-BthA-I monomer B and m-BthA-I. The average *B* factors for m-BthA-I and d-BthA-I are 25.6 and 18.6 $Å^2$, respectively (calculated without solvent molecules).

In the active site for both structures, there is just a water molecule bound to His48 and Lys49 residues.

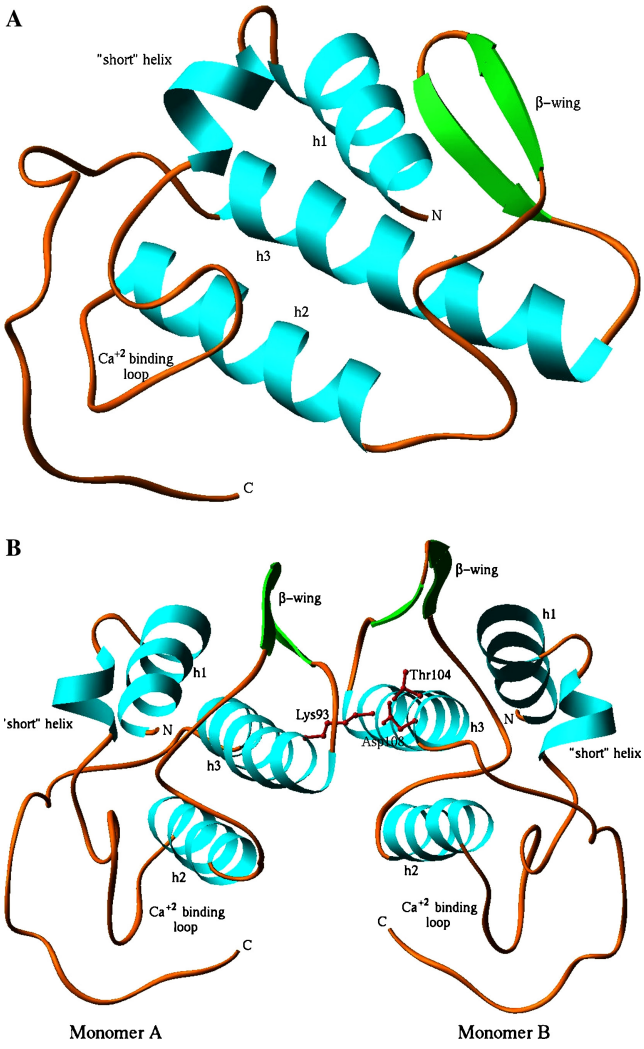

Fig. 1. Structures of (A) m-BthA-I and (B) d-BthA-I are showed as a ribbon diagram [35]. The residues Thr104, Asp108, and Lys93 of interface of monomers of d-BthA-I are shown in a ball-stick representation.

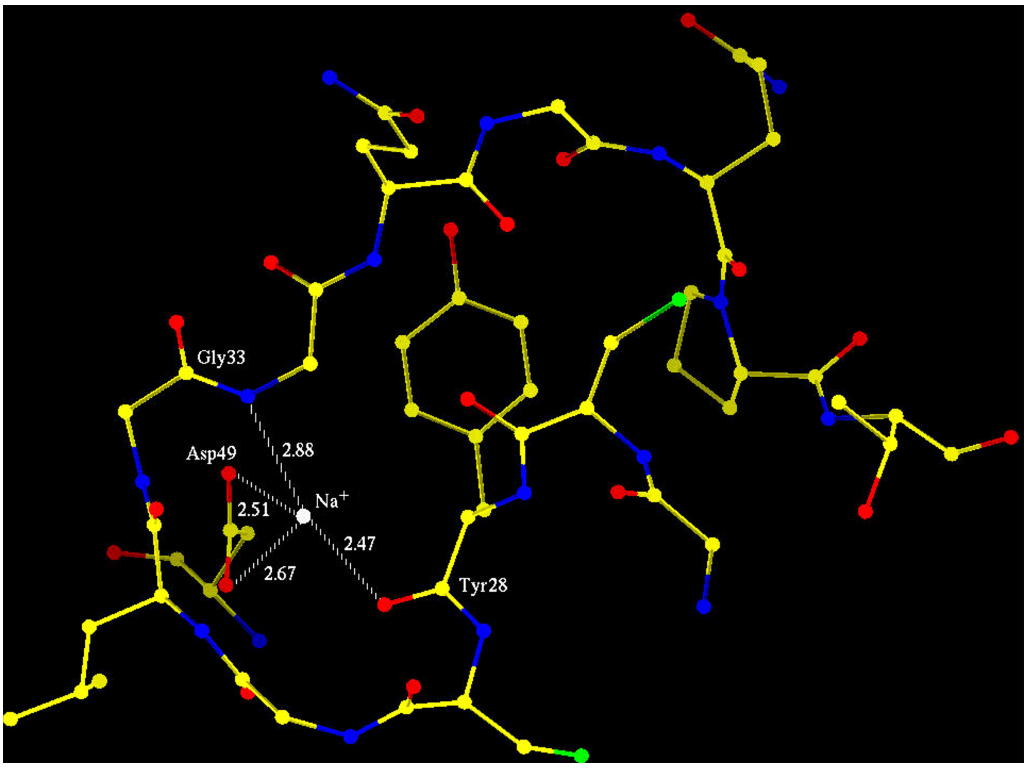

Fig. 2. Ca^{2+}-binding loop interactions with Na^{+} ion in the m-BthA-I structure [31].

The electron density map for m-BthA-I structure shows a single prominent peak at the center of Ca^{2+}-binding site, which was identified as Na^{+} ion rather than Ca^{2+} ion for three main reasons. (i) The protein was crystallized in the presence of sodium acetate. (ii) The *B* factor of Na^{+} is 38.1 $Å^2$, which is reasonably close to the value of the average *B* factor (23.2 $Å^2$). If the position was occupied by Ca^{2+} ion, its *B* factor would be 60.3 $Å^2$. (iii) All PLA_2s solved to this time with the presence of Ca^{2+} present this ion coordinated by carboxyl group of residues 28, 30, 32, and Asp49 and two (or one) water molecules [36]. However, the Na^{+} ion of m-BthA-I just interacts with the Tyr28 carboxyl group (2.47 Å), Gly32 N (2.88 Å), and Asp49 Oδ1 and Oδ2 (2.67 and 2.51 Å, respectively) (Fig. 2). Additionally, the distance between the closest water molecule and the Na^{+} ion is about 4 Å, which makes impossible the essential role of a water molecule presence in the catalytic mechanism [37].

No strong densities were found at the center of Ca^{2+}-binding loops of d-BthA-I monomers. However, water molecules were found in both sites of d-BthA-I in the similar position to the Na^{+} ion of m-BthA-I (*B* factors are 33.9 and 43.5 $Å^2$ which are comparable with the average value of 40.9 $Å^2$ for water molecules). Despite the lack of Na^{+} ion in the d-BthA-I, the conformations of Ca^{2+}-binding loops are similar with m-BthA-I molecule (superposition between the m-BthA-I

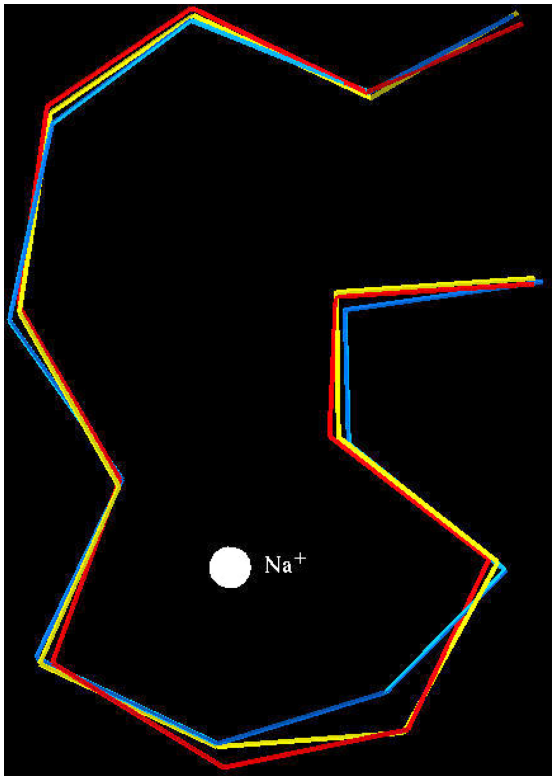

Fig. 3. Superposition of C^{α} atoms of Ca^{2+}-binding loop of each one monomer of d-BthA-I (red, monomer A; blue, monomer B) and m-BthA-I. Na^{+} ion is shown like a white sphere [31]. (For interpretation of the references to color, the reader is referred to the web version of this paper.)

loop and d-BthA-I monomers A and B loops resulted in C^{α} atom r.m.s. deviation of 0.26 and 0.46 Å, respectively) (Fig. 3).

The monomers of d-BthA-I are related by twofold axis perpendicular to h3 α-helix (Fig. 1B). Hydrophobic contacts, one intermolecular hydrogen bond, and one

```
                                10        20        30        40        50        60          Identity (%)
B. taurus (1bp2)          ALWQFNGMIKCKIPSSEPLLDFNNYGCYCGLGGSGTPVDDLDRCCQTHDNCYKQAKKLDSCKVLVDNPY      41.6
B. jararacussu (1umv)     SLWQFGKMINYVM-GESGVLQYLSYGCYCGLGGQGQPTDATDRCCFVHDCCYG---KVTGC-----NPK       -
A. p. piscivorus (1vap)   NLFQFEKLIKKMT-GKSGMLWYSAYGCYCGWGGQGRPKDATDRCCFVHDCCYG---KVTGC-----DPK      71.5
D. acutus (1ijl)          SLIQFETLIMKVV-KKSGMFWYSAYGCYCGWGGHGRPQDATDRCCFVHDCCYG---KVTGC-----NPK      66.7
C. atrox (1pp2)           SLVQFETLIMKIA-GRSGLLWYSAYGCYCGWGGHGLPQDATDRCCFVHDCCYG---KATDC-----DPK      63.1
A. h. pallas (1jia)       HLLQFRKMIKKMT-GKEPVVSYAFYGCYCGSGGRGKPKDATDRCCFVHDCCYE---KVTGC-----KPK      62.8
B. pirajai (1gmz)         DLWQFGKMILKET-GKLPFPYYVTYGCYCGVGGRGGPKDATDRCCFVHDCCYG---KLTSC-----NPK      59.5
D. r. pulchella (1fb2)    SLLEFGKMILEET-GKLAIPSYSSYGCYCGWGGKGTPKDATDRCCFVHDCCYG---NLPDC-----NPK      54.3
N. n. sagittifera (1mh2)  NTWQFKNMISCTVPSR-SWWDFADYGCYCGRGGSGTPSDDLDRCCQTHDNCYNEAEKISGC-VLVDNPR      41.8

                                70        80        90       100       110       120
B. taurus (1bp2)          TNNYSYSCSNNEITCSS-ENNACEAFICNCDRNAAICF-----SKVPYNKE-HKNLDKKNC-------      41.6
B. jararacussu (1umv)     IDSYTYSKKNGDVVCGG-DN-PCKKQICECDRVATTCFRD---NKDTYDIK-YWFYGAKNCQEKSEPC       -
A. p. piscivorus (1vap)   MDIYTYSVDNGNIVCGG-TN-PCKKQICECDRAAAICFRD---NLKTYDSKTYWKYPKKNCKEESEPC      71.5
D. acutus (1ijl)          MDSYTYSEENGDIVCGG-DD-PCKREICECDRVAADCFRD---NLDTYNSDTYWRYPRQDCEESPEPC      66.7
C. atrox (1pp2)           TVSYTYSEENGEIICGG-DD-PCGTQICECDKAAAICFRD---NIPSYDNK-YWLFPPKDCREEPEPC      63.1
A. h. pallas (1jia)       WDDYTYSWKNGTIVCGG-DD-PCKKEVCECDKAAAICFRD---NLKTYKKR-YMAYPDILCSSKSEKC      62.8
B. pirajai (1gmz)         TDRYSYSRKDGTIVCGE-D--PCRKEICECDKAAAVCFRE---NLDTYNKK-YMSYLKSLCK-KADDC      59.5
D. r. pulchella (1fb2)    SDRYKYKRVNGAIVCEK-GT-SCENRICECDKAAAICFRQ---NLNTYSKK-YMLYPDFLCKGELKC-      54.3
N. n. sagittifera (1mh2)  FRTYSYACTAGTLTCTGRNN-ACAASVCDCDRNAAICFAGAPYNDSNYNID-LQARCN----------      41.8

Key: red = helix, blue = strand, green = turn, black = coil.
```

Fig. 4. Amino acid sequence alignments of Asp49-PLA_2s monomers A from *B. jararacussu* (1u73), *A. p. piscivorus* (1vap) [29], *D. acutus* (1ijl) [39], *C. atrox* (1pp2) [40], *A. h. pallas* (1jia) [41], *D. r. pulchella* (1fb2) [42], and *N. n. sagittifera* (1mh2—monomer B) [43]. The sequences have been numbered according to Renetseder et al. [44]. Identity values related to BthA-I are shown at the right column. Produced by the FASTA program [45]. PDB ID codes are shown in parentheses.

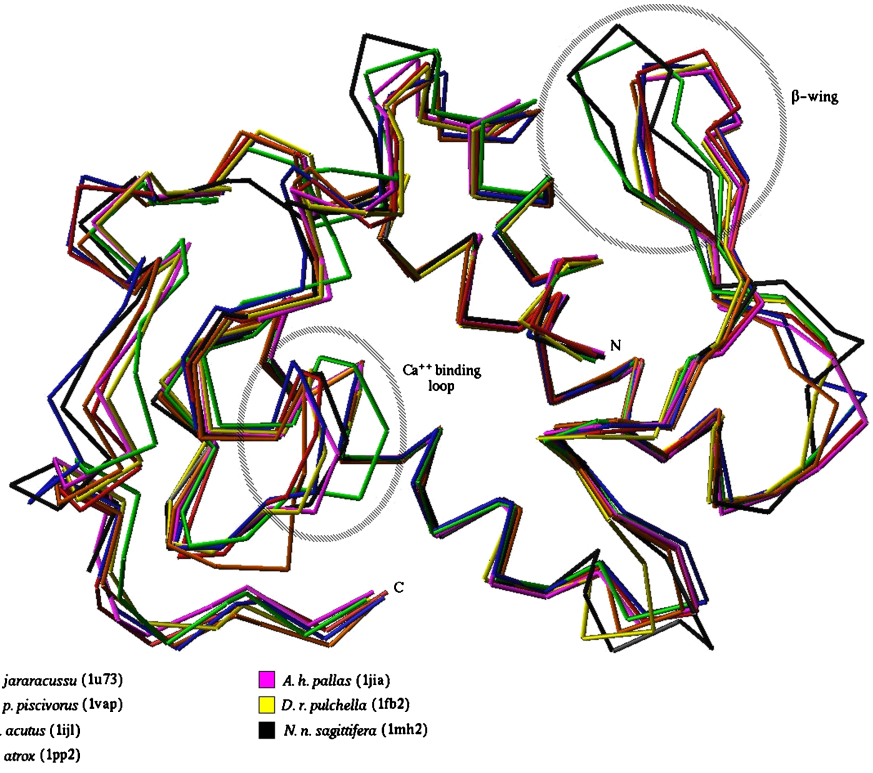

Fig. 5. Superposition of monomers A Asp49-PLA_2s from *B. jararacussu* (1u73), *A. p. piscivorus* (1vap) [29], *D. acutus* (1ijl) [39], *C. atrox* (1pp2) [40], *A. h. pallas* (1jia) [41], *D. r. pulchella* (1fb2) [42], and *N. n. sagittifera* (1mh2—monomer B) [43]—performed using only C^{α} atoms from h1, h2, and h3 α-helixes [31]. Asp49-PLA_2 from the *N. n. sagittifera* venom belongs to group I while the others to the group IIA. Drawn using RIBBONS [35]. PDB ID codes are shown in parentheses.

salt-bridge contribute to the stabilization of the dimer. All contacts involve the residues of h3 α-helix, including the salt bridge between the Nε atom of Lys83 (monomer A) and Oδ2 of Glu98 (monomer B) (2.56 Å).

Discussion

It was identified to be a Na^+ ion rather of a Ca^{2+} ion for m-BthA-I at the center of Ca^{2+}-binding site. Similar fact was observed in the acidic PLA_2 structure from *Agkistrodon halys pallas* complexed with *p*-bromo-phenacyl (BPB) [38], which was crystallized in the presence of Na^+ ions. Zhao et al. [38] noted the strong interaction of Na^+ ion with three carbonyl oxygen atoms of residues Tyr28, Gly 30, and Gly32 while for Asp49 Oδ1 and Oδ2 these interactions are longer than usual. In the case of m-BthA-I, Na^+ ion interacts with Tyr28 carboxyl, Gly32 N, and Asp49 Oδ1 and Oδ2. These differences are likely to be due to the *p*-bromo-phenacyl group interacting with Gly30 and Asp49 in the PLA_2 structure from *A. h. pallas* complexed with BPB [38].

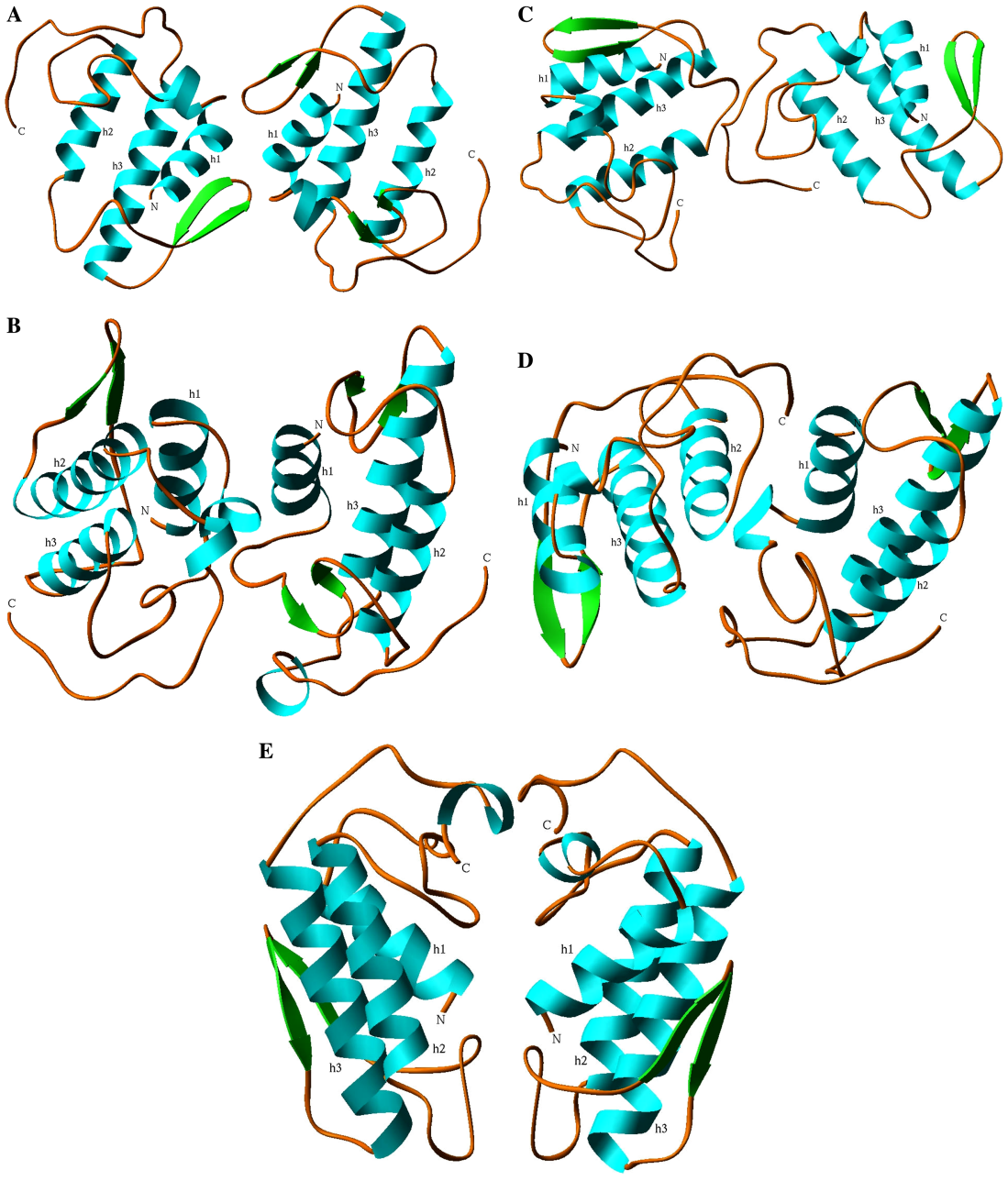

Fig. 6. Structure of dimeric PLA_2s: (A) *Bothrops neuwiedi pauloensis* (1pa0) [12]; (B) *Deinagkistrodon acutus* (1ijl) [39]; (C) *Agkistrodon halys pallas* (1jia) [41]; (D) *Daboia russeli pulchella* (1fb2) [42]; and (E) *Naja naja sagittifera* (1mh2) [43]. Drawn using RIBBONS [35]. PDB ID codes are shown in parentheses.

The d-BthA-I structure shows the lack of Ca^{2+} or Na^{+} ions at the Ca^{2+}-binding loops, however, a water molecule was found in similar position for both monomers. The Ca^{2+}-binding loops do not show important structural differences by occupation of this site by water or Na^{+} ion (Fig. 3).

Fig. 4 shows the alignment of the class I or IIA Asp49-PLA_2s from different species (*B. jararacussu*, *A. p. piscivorus* [29], *Deinagkistrodon acutus* [39], *Crotalus atrox* [40], *A. h. pallas* [41], *Daboia russeli pulchella* [42], and *Naja naja sagittifera* [43]) produced using only the secondary structure residues. The sequence identity related to BthA-I varies from 71.5% (*A. p. piscivorus*) to 41.8% (*N. n. sagittifera*). In contrast, the C^{α} atom's superposition of secondary structure elements between monomers (Fig. 5) shows conformations to be very similar. As seen in Fig. 5, the main structural differences are in the Ca^{2+}-binding loop and β-wing regions. BthA-I presents these regions as slightly altered compared to other class IIA PLA_2 (all structures of Fig. 5, except the class I Asp49-PLA_2 from the *N. n. sagittifera*). In contrast, in the Asp49-PLA_2 piratoxin III structure [18], Ca^{2+}-binding loop presents high structural distortion when compared with other PLA_2s due to an extreme diversion taken by the main chain of residues 30–31 associated with a change in the backbone dihedral angles of Cys29. The authors support this distortion may be due to an alternative conformation of enzyme (T-state). In that case, the structures of BthA-I and other PLA_2s presented here should be in the R-state conformation.

The oligomeric state is an important issue for many of phospholipase A_2 structures solved [12,37,46–49]. A comparison of d-BthA-I with all class IIA PLA_2 structures available at the RCSB Protein Data Bank reveals this structure adopts a novel oligomeric conformation whereas the active site of both monomers can be reached by a hydrophobic channel exposed to the solvent. Fig. 6 shows some examples of oligomeric conformations of PLA_2s.

BthA-I was crystallized in two conformational states: monomeric and dimeric. This is likely to be due to the physicochemical conditions used in the crystallization experiments. The crystals of m-BthA-I were grown at pH 4.6 and those of d-BthA-I were grown at pH 3.5. Then, the m-BthA-I molecules are in the condition very close to their p$I \sim 5.0$ [24], whereas the molecules are in charge equilibrium leading to their dissociation. Consequently, we suggest dimeric state of BthA-I could be that found predominately in vivo.

It has been shown dimeric is the most favorable or active state for Lys49-PLA_2 [12,46] and for outer membrane phospholipases (OMPLA) [47,48]. However, *C. atrox* PLA_2 is dimeric in the absence of lipids and monomeric when interacting with lipids [49]. Then, clearly, deep structural studies must be done to better understanding of oligomeric mechanism Asp49-PLA_2s.

Acknowledgments

The authors gratefully acknowledge the financial support from Fundação de Amparo à Pesquisa do Estado de São Paulo (FAPESP), Conselho Nacional de Desenvolvimento Científico e Tecnológico (CNPq), Fundação para o Desenvolvimento da UNESP (FUNDUNESP), Laboratório Nacional de Luz Síncrontron (LNLS, Campinas-SP), and Universidade de Ribeirão Preto (UNAERP, Ribeirão Preto-SP).

References

[1] D.A. Six, E.A. Dennis, The expanding superfamily of phospholipase A_2 enzymes: classification and characterization, Biochim. Biophys. Acta 1488 (2000) 1–19.
[2] P. Rosenberg, in: W. Shier, D. Mebs (Eds.), Handbook of Toxinology, Marcel Dekker, New York, 1990, pp. 67–277.
[3] J.M. Gutiérrez, B. Lomonte, Phospholipase A_2 myotoxins from *Bothrops* snake venoms, in: R.M. Kini (Ed.), Venom Phospholipase A_2 Enzymes: Structure, Function and Mechanism, Wiley, Chichester, 1997, pp. 321–352.
[4] C.L. Ownby, Structure, function and biophysical aspects of the myotoxins from snake venoms, J. Toxicol. Toxin Rev. 17 (1998) 1003–1009.
[5] E. Valentin, G. Lambeau, What can venom phospholipase A_2 tell us about the functional diversity of mammalian secreted phospholipase A_2, Biochimie 82 (2000) 815–831.
[6] R.M. Kini, H.J. Evans, A model to explain the pharmacological effects of snake venom phospholipases A_2, Toxicon 27 (1989) 613–635.
[7] A.M. Soares, J.R. Giglio, Chemical modifications on phospholipases A_2 from snake venoms: effects on catalytic and pharmacological properties. Review, Toxicon 42 (2004) 855–868.
[8] P. Needleman, J. Turk, B.A. Jakschik, A.R. Morrison, J.B. Lefkowith, Arachidonic acid metabolism, Annu. Rev. Biochem. 55 (1986) 69–102.
[9] B. Francis, J.M. Gutierrez, B. Lomonte, I.I. Kaiser, Myotoxin II from *Bothrops asper* (terciopelo) venom in a lysine-49 phospholipase A_2, Arch. Biochem. Biophys. 284 (1991) 352–359.
[10] C.L. Ownby, H.S. Selistre de Araújo, S.P. White, J.E. Fletcher, Lysine 49 phospholipases A2 proteins. Review, Toxicon 37 (1999) 411–445.
[11] D.L. Scott, A. Achari, J.C. Vidal, P.B. Sigler, Crystallographic and biochemical studies of the (inactive) Lys49 phospholipase A_2 from the venom of *Agkistrodon piscivorus piscivorus*, J. Biol. Chem. 267 (1992) 22645–22657.
[12] A.J. Magro, A.M. Soares, J.R. Giglio, M.R.M. Fontes, Crystal structures of BnSP-7 and BnSP-6, two Lys49-phospholipases A_2: quaternary structure and inhibition mechanism insights, Biochem. Biophys. Res. Commun. 311 (2003) 713–720.
[13] A.M. Soares, M.R. Fontes, J.R. Giglio, Phospholipase A_2 myotoxins from *Bothrops* snake venoms: structure–function relationship, Curr. Org. Chem. 8 (2004) in press.
[14] W.F. de Azevedo Jr., R.J. Ward, F.R. Lombardi, J.R. Giglio, A.M. Soares, M.R.M. Fontes, R.K. Arni, Crystal structure of myotoxin-II: a myotoxic phospholipase A2 homologue from *Bothrops moojeni* venom, Protein Pept. Lett. 4 (1997) 329–334.
[15] M.T. da Silva-Giotto, R.C. Garrat, G. Oliva, Y.P. Mascarenhas, J.R. Giglio, A.C.O. Cintra, W.F. de Azevedo Jr., R.K. Arni, R.J. Ward, Crystallographic and spectroscopic characterization of a molecular hinge: conformational changes in bothropstoxin I, a

dimeric Lys49-phospholipase A_2 homologue, Proteins: Struct. Funct. Genet. 30 (1998) 442–454.
[16] W.H. Lee, M.T. da Silva-Giotto, S. Marangoni, M.H. Toyama, I. Polikarpov, R.C. Garratt, Structural basis for low catalytic activity in Lys49-phospholipase A_2—a hypothesis: the crystal structure of piratoxin II complexed to fatty acid, Biochemistry 40 (2001) 28–36.
[17] R.K. Arni, M.R.M. Fontes, C. Barberato, J.M. Gutiérrez, C. Díaz-Oreiro, R.J. Ward, Crystal structure of myotoxin II, a monomeric Lys49-phospholipase homologue isolated from the venom of *Cerrophidion* (*Bothrops*) *godmani*, Arch. Biochem. Biophys. 366 (1999) 177–182.
[18] S.H. Andrião-Escarso, A.M. Soares, V.M. Rodrigues, Y. Angulo, C. Diaz, B. Lomonte, J.M. Gutiérrez, J.R. Giglio, Myotoxic phospholipases A_2 in *Bothrops* snake venoms: effect of chemical modifications on the enzymatic and pharmacological properties of bothropstoxins from *Bothrops jararacussu*, Biochimie 82 (2000) 755–763.
[19] D.J. Rigden, L.W. Hwa, S. Marangoni, M.H. Toyama, I. Polikarpov, The structure of the D49 phospholipase A_2 piratoxin III from *Bothrops pirajai* reveals unprecedented structural displacement of the calcium-binding loop: possible relationship to cooperative substrate binding, Acta Crystallogr. D 59 (2003) 255–262.
[20] J.J. Daniele, I.D. Bianco, G.D. Fidelio, Kinetic and pharmacological characterization of phospholipases A_2 from *Bothrops neuwiedii* venom, Arch. Biochem. Biophys. 318 (1995) 65–70.
[21] S.M.T. Serrano, A.P. Reichl, R. Mentele, E.A. Auerswald, M.L. Santoro, C.A.M. Sampaio, A.C.M. Camargo, M.T. Assakura, A novel phospholipase A2, BJ-PLA2, from the venom of the snake *Bothrops jararaca*: purification, primary structure analysis, and its characterization as a platelet-aggregation-inhibiting factor, Arch. Biochem. Biophys. 367 (1999) 26–32.
[22] M.I. Homsi-Brandeburgo, L.S. Queiroz, H. Santo-Neto, L. Rodrigues-Simioni, J.R. Giglio, Fractionation of *Bothrops jararacussu* snake venom: partial chemical characterization and biological activity of bothropstoxin, Toxicon 26 (1988) 615–627.
[23] M.F. Pereira, J.C. Novello, A.C.O. Cintra, J.R. Giglio, E.C.T. Landucci, B. Oliveira, S. Marangoni, The amino acid sequence of bothropstoxin-II, an Asp-49 myotoxin from *Bothrops jararacussu* (jararacucu) venom with low phospholipase A_2 activity, J. Protein Chem. 17 (1998) 381–386.
[24] S.H. Andrião-Escarso, A.M. Soares, M.R.M. Fontes, A.L. Fuly, F.M.A. Corrêa, J.C. Rosa, L.J. Greene, J.R. Giglio, Structural and functional characterization of an acidic platelet aggregation inhibitor and hypotensive phospholipase A_2 from *Bothrops jararacussu* snake venom, Biochem. Pharmacol. 64 (2002) 723–732.
[25] P.G. Roberto, S. Kashima, S. Marcussi, J.O. Pereira, S. Astolfi-Filho, A. Nomizo, J.R. Giglio, M.R.M. Fontes, A.M. Soares, S.C. França, Cloning and identification of a complete cDNA coding for a bactericidal and antitumoral acidic phospholipase A_2 from *Bothrops jararacussu* venom, Protein J. 23 (2004) 273–285.
[26] P.G. Roberto, S. Kashima, A.M. Soares, L. Chioato, V.M. Faça, A.L. Fuly, S. Astolfi-Filho, J.O. Pereira, S.C. França, Cloning and expression of an acidic platelet aggregation inhibitor phospholipase A_2 cDNA from *Bothrops jararacussu* venom gland, Protein Expr. Purif. 37 (2004) 102–108.
[27] Z. Otwinowski, W. Minor, Processing of X-ray diffraction data collected in oscillation mode, Methods Enzymol. 276 (1997) 307–326.
[28] J. Navaza, AMoRe: an automated package for molecular replacement, Acta Crystallogr. A50 (1994) 157–163.
[29] S.K. Han, E.T. Yoon, D.L. Scott, P.B. Sigler, W. Cho, Structural aspects of interfacial adsorption. A crystallographic and site-directed mutagenesis study of the phospholipase A2 from the venom of *Agkistrodon piscivorus piscivorus*, J. Biol. Chem. 272 (1997) 3573–3582.
[30] A.T. Brünger, P.D. Adams, G.M. Clore, W.L. DeLano, P. Gros, R.W. Grosse-Kunstleve, J.S. Jiang, J. Kuszewski, M. Nilges, N.S. Pannu, R.J. Read, L.M. Rice, T. Simonson, G.L. Warren, Crystallography and NMR system (CNS): a new software system for macromolecular structure determination, Acta Crystallogr. D54 (1998) 905–921.
[31] T.A. Jones, M. Bergdoll, M. Kjeldgaard, O: a macromolecule modeling environment, in: C.E. Bugg, S.E. Ealick (Eds.), Crystallographic and Modeling Methods in Molecular Design, Springer-Verlag, New York, 1990, pp. 189–195.
[32] A.T. Brünger, X-PLOR Version 3.1: A System for Crystallography and NMR, Yale University Press, New Haven, 1992.
[33] Collaborative Computing Project No. 4 (CCP4), The CCP4 suite: programs for protein crystallography, Acta Crystallogr. D 50 (1994) 760–763.
[34] R.A. Laskowski, M.W. MacArthur, D.S. Moss, J.M. Thornton, Procheck: a program to check the stereochemical quality of protein structures, J. Appl. Crystallogr. 26 (1993) 283–291.
[35] M. Carson, Ribbons, Methods Enzymol. 277 (1997) 493–505.
[36] S. Xu, L. Gu, T. Jiang, Y. Zhou, Z. Lin, Structures of cadmium-binding acidic phospholipase A_2 from the venom of *Agkistrodon halys* Pallas at 1.9 Å resolution, Biochem. Biophys. Res. Commun. 300 (2003) 271–277.
[37] Y.H. Pan, T.M. Epstein, M.K. Jain, B.J. Bahnson, Five coplanar anion binding sites on one face of phospholipase A_2: relationship to interface binding, Biochemistry 40 (2001) 609–617.
[38] H. Zhao, T. Liang, W. Xiaoqiang, Z. Yuancong, L. Zhengjiong, Structure of a snake venom phospholipase A_2 modified by *p*-bromo-phenacyl-bromide, Toxicon 36 (1998) 875–886.
[39] L. Gu, H. Zhang, S. Song, Y. Zhou, Z. Lin, Structure of an acidic phospholipase A2 from the venom of *Deinagkistrodon acutus*, Acta Crystallogr. D 58 (2002) 104–110.
[40] S. Brunie, J. Bolin, D. Gewirth, P.B. Sigler, The refined crystal structure of dimeric phospholipase A2 at 2.5 Å. Access to a shielded catalytic center, J. Biol. Chem. 260 (1985) 9742–9749.
[41] V. Chandra, P. Kaur, J. Jasti, C. Betzel, T.P. Singh, Regulation of catalytic function by molecular association: structure of phospholipase A2 from *Daboia russelli pulchella* (DPLA2) at 1.9 Å resolution, Acta Crystallogr. D 57 (2001) 1793–1798.
[42] K. Zhao, S. Song, Z. Lin, Y. Zhou, Structure of a basic phospholipase A2 from *Agkistrodon halys* Pallas at 2.13 Å resolution, Acta Crystallogr. D 510 (1998) 510–521.
[43] T. Jabeen, A.K. Varma, M. Paramasivam, N. Singh, R.K. Singh, S. Sharma, A. Srinivasan, T.P. Singh, Crystal structure of a zinc containing dimer of phospholipase A2 from the venom of Indian cobra (*Naja naja saggittifera*), to be published.
[44] R. Renetseder, S. Brunie, B.W. Dijkstra, J. Drenth, P.B. Sigler, A comparison of the crystal structures of phospholipases A_2 from bovine pancreas and *Crotalus atrox* venom, J. Biol. Chem. 260 (1985) 11627–11636.
[45] W.R. Pearson, Rapid and sensitive sequence comparison with FASTP and FASTA, Methods Enzymol. 183 (1990) 63–98.
[46] A.H. de Oliveira, J.R. Giglio, S.H. Andrião-Escarso, A.S. Ito, R.J. Ward, A pH-induced dissociation of the dimeric form of a lysine 49-phospholipase A_2 abolishes Ca^{2+}-independent membrane damaging activity, Biochemistry 40 (2001) 6912–6920.
[47] N. Dekker, Outer-membrane phospholipase A: known structure, unknown biological function, Mol. Microbiol. 35 (2000) 711–717.
[48] H.J. Snijder, I. Ubarretxena-Belandia, M. Blaauw, K.H. Kalk, H.M. Verheij, M.R. Egmond, N. Dekker, B.W. Dijkstra, Structural evidence for dimerization-regulated activation of an integral membrane phospholipase, Nature 401 (1999) 717–721.
[49] S.A. Sanchez, Y. Chen, J.D. Muller, E. Gratton, T.L. Hazlett, Solution and interface aggregation states of *Crotalus atrox* venom phospholipase A_2 by two-photon excitation fluorescence correlation spectroscopy, Biochemistry 40 (2001) 6903–6911.